Cellulose (2020) 27:693–702
https://doi.org/10.1007/s10570-019-02822-1

ORIGINAL RESEARCH

Fabrication of ultrastiff and strong hydrogels by in situ polymerization in layered cellulose nanofibers

Xianpeng Yang · Subir K. Biswas · Hiroyuki Yano · Kentaro Abe

Received: 21 August 2019 / Accepted: 28 October 2019 / Published online: 4 November 2019

Abstract Integrating high stiffness, strength, and toughness on par with those of soft tissues into synthetic hydrogels is extremely challenging. We have proposed a method to overcome this problem: in situ polymerization of a polymer matrix in layered cellulose nanofibers. In an attempt, ionically cross-linked poly(acrylamide-co-acrylic acid) is fabricated in a wet cellulose nanofiber cake. The resulting hydrogels, called ionically cross-linked nanocomposite (ICN) hydrogels, exhibit a readily adjustable elastic modulus (11.9–190.0 MPa) and high fracture strength (generally $>$ 10 MPa), which are comparable with those of skin and ligament. The high frictional force between the cellulose nanofibers and matrix is responsible for the stiffness of ICN hydrogels; while the tough matrix and weak direct interfibrillar interactions enable good stretchability. We expect that various kinds of cellulose nanofiber/polymer nanocomposite hydrogels with excellent mechanical properties and/or other features can be fabricated by simply changing the monomers.

Keywords Nanocomposite hydrogels · Cellulose nanofibers · In situ polymerization · Tensile properties · Versatility

Introduction

Many soft tissues, such as skin and ligament, are wet materials but have excellent load-bearing properties (Wegst and Ashby 2004; Meyers et al. 2008). For example, skin and ligament, which contain more than 60% water, have extremely high tensile stiffness (elastic moduli of 10 to several hundred MPa) and strength (fracture strength of more than 10 MPa) (Wegst and Ashby 2004; Dubinskaya et al. 2007). Synthesized hydrogels have similar wet properties to soft tissues, and they have attractive application prospects in soft tissue replacement (Gong 2010; Wang et al. 2017; Zhang and Khademhosseini 2017). Load-bearing hydrogels have attracted much attention in the last few decades, but very few hydrogels reach the stiffness and strength of load-bearing tissues (Wang et al. 2017; Zhang and Khademhosseini 2017; Mredha et al. 2018). Integrating high stiffness,

Electronic supplementary material The online version of this article (https://doi.org/10.1007/s10570-019-02822-1) contains supplementary material, which is available to authorized users.

X. Yang (✉) · S. K. Biswas · H. Yano · K. Abe (✉)
Research Institute for Sustainable Humanosphere, Kyoto University, Gokasho, Uji, Kyoto 611-0011, Japan
e-mail: yang.xianpeng.84z@st.kyoto-u.ac.jp

K. Abe
e-mail: abekentaro@rish.kyoto-u.ac.jp

S. K. Biswas
e-mail: subir.biswas.88a@st.kyoto-u.ac.jp

H. Yano
e-mail: yano@rish.kyoto-u.ac.jp

strength, and toughness, which are interrelated for synthesized hydrogels, remains elusive (Li et al. 2014; Zhao 2017).

Cellulose nanofibers (CNFs), a nature-based hydrophilic material, have high estimated tensile modulus and strength comparable with steel and Kevlar fibers (Klemm et al. 2011). Dried CNF sheets, with various resources of cellulose, also show an elastic modulus around 11 GPa and fracture strength more than 200 MPa (Abe and Yano 2009a, b). Thus, two types of CNF-based load-bearing hydrogels have been developed: CNF-only hydrogels and CNF/polymer composite hydrogels (De France et al. 2017; Nascimento et al. 2018). CNF-only hydrogels, comprising high content of CNFs, show high stiffness (Abe and Yano 2012). However, they are generally not stretchable owing to the rigid cellulose chains. For CNF/polymer composite hydrogels, they are prepared from CNF suspensions and can be highly stretchable (De France et al. 2017; Nascimento et al. 2018; Kobe et al. 2016). However, the CNF content is generally less than 2.5% because of the high viscosity of CNFs, limiting the reinforcement (De France et al. 2017; Chen et al. 2018). Furthermore, the macroscopic mechanical properties of CNFs are dramatically reduced in wet condition, which is due to the dissociation of the interfibrillar hydrogen bonds (Benitez et al. 2013).

We recently reported a CNF/polyvinyl alcohol (PVA) composite hydrogel with a high CNF content from a layered CNF cake which was obtained by filtrating a dilute CNF suspension (Yang et al. 2018). The strong interactions between the CNFs and PVA chains inhibit deformation, while the PVA network and weak interfibrillar interactions enable good stretchability, resulting in simultaneous high stiffness, strength and toughness. However, it is difficult to control the diffusion of viscous polymer solution into the layered CNFs, limiting the content and types of polymers. In the current work, to increase the above method by one step, we try to in situ polymerize the polymer matrix in a CNF cake. Polyacrylamide has been widely used to prepare hydrogel because of hydrophilic, biocompatible and atoxic properties (Oyen 2013). In addition, partial grafting of polymer chains on the surfaces of CNFs occur with persulfate as initiator, which contributes to toughness of composite hydrogels (Mahfoudhi and Boufi 2016). On the other hand, polyacrylamide chain is very flexible (Chen et al. 2018; Mahfoudhi and Boufi 2016). To increase the interactions between CNFs and polymer matrix, we used acrylic acid as comonomer which can be ionically cross-linked after polymerization (Lin et al. 2015; Hu et al. 2016; Zheng et al. 2016; Lin et al. 2016). Thus, ionically cross-linked poly(acrylamide-co-acrylic acid) (poly(AM-co-AA)) was fabricated as a model matrix in the current research. The tensile properties of the composite hydrogels and the corresponding fracture mechanism are discussed.

Experimental section

Materials

Acrylic acid (AA, $\geq$ 99%) was purchased from Sigma-Aldrich (Osaka, Japan). The other chemicals were obtained from Wako Pure Chemicals (Osaka, Japan). All of the chemicals were laboratory grade and used as received. The CNFs were prepared according to our previous study (Abe et al. 2007; Yang et al. 2018). Briefly, Japanese cypress wood powder was chlorite- and alkali- treated to remove lignin and hemicellulose, respectively. The CNFs were obtained by passing a pulp suspension, with a concentration of around 0.8 wt%, through an MKCA6-3 grinder (Masuko Sangyo Corp., Saitama, Japan). The CNFs possessed a uniform diameter of around 15 nm (Fig. S1).

Preparation of the CNF/poly(AM-co-AA) hydrogels

A total of 200 mL of the CNF suspension with a concentration of 0.1 wt% was vacuum filtrated using a filter holder with an inner diameter of 75 mm to form a wet CNF cake with thickness of around 0.5 mm (Fig. 1a). A solution (3 mL) containing acrylamide (AM) and AA as monomers, ammonium persulfate (APS) as an initiator, and methylene-bis-acrylamide (MBA) as a covalent cross-linker was then filtrated through the CNF cake to replace water (Fig. 1b). The above replacement process was repeated three times. The filtration of the CNF suspension and monomer solution required about 70 min and 10 min, respectively. The concentrations of both the initiator and covalent cross-linker were fixed at 0.1 mol% with respect to the total monomers, unless otherwise stated.

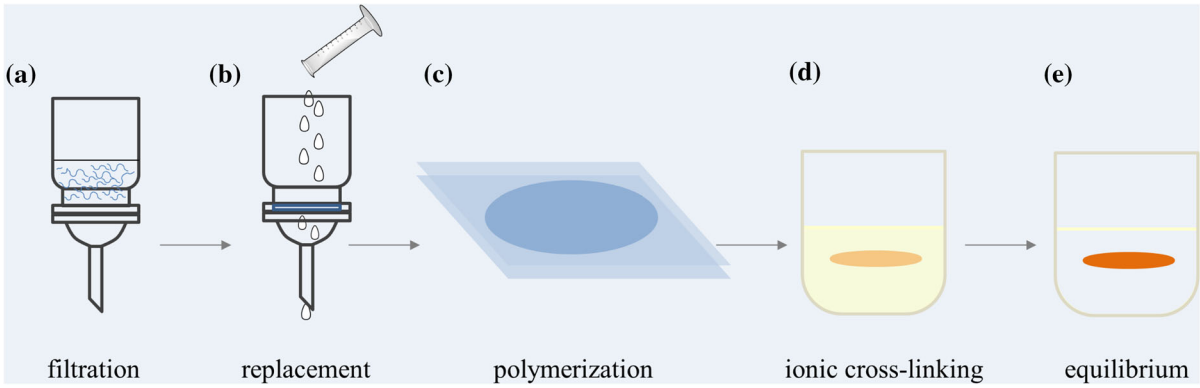

Fig. 1 Preparation of the ICN hydrogels. **a** A CNF suspension was filtrated to form a CNF cake. **b** Water in the CNF cake was replaced by passing a monomer solution through the nanochannels inside the cake. **c** In situ polymerization of poly(AM-co-AA) in the CNF cake was performed. **d** Poly(AM-co-AA) was ionically cross-linked by Fe^{3+}. **e** Excess Fe^{3+} was washed out by equilibration in water

The water-replaced CNF cake was fixed between two glass slides and sealed. Polymerization was performed at 80 °C for 12 h to form a as-prepared CNF/(AM-co-AA) hydrogel (Fig. 1c).

Preparation of the ionically cross-linked nanocomposite hydrogels

The as-prepared CNF/poly(AM-co-AA) hydrogel was immersed in $FeCl_3$ solution for 24 h to perform ionic cross-linking (Fig. 1d). The concentration of $FeCl_3$ was fixed at 0.06 mol/L. After ionic cross-linking, the hydrogel was immersed in water to remove excess ions (Fig. 1e). The resulting hydrogels are called ionically cross-linked nanocomposite (ICN) hydrogels. The ratio of AA to the total monomers and the concentration of total monomers were investigated in detail. In the following, AA-*m*% means that the molar ratio of AA to total monomers was *m*%, while the molar concentration of total monomers to water was fixed at 3 mol/L. For example, AA-8% was prepared from a 3 mol/L solution of monomers containing 8 mol% AA. *n*-M means that the molar concentration of total monomers to water was *n* mol/L, while the molar ratio of AA to total monomers was fixed at 20%. For example, 1.5-M was prepared from a 1.5 mol/L solution of monomers containing 20 mol % AA.

Mechanical tests

All of the mechanical tests were performed with a universal testing machine (model 3365, Instron Corp., Canton, MA) equipped with a 2 kN cell at a stretching velocity of 20 mm/min. For the tensile tests, dumbbell-shaped samples (width 2 mm, length 35 mm, gauge length 20 mm) were used. Five specimens were analyzed. The elastic moduli were determined from the initial slopes of the tensile stress–strain curves (0%–1% strain). Rectangular species (width 5 mm, length 20 mm, gauge length 10 mm) were used for the single edge crack tests, which was the same with our previous report (Yang et al. 2018).

Water content

The hydrogels were dried in an oven at 110 °C overnight. The water contents of the hydrogels were calculated by

$$\text{water content} = \frac{W_w - W_d}{W_w} \times 100\%,$$

where W_w is the weight of the hydrogels after equilibration in water and W_d is the weight after complete drying.

Structural characterization

The SEM images were obtained with a JSM-7800F Prime field-emission scanning electron microscope (JEOL, Tokyo, Japan) at an acceleration voltage of 5 kV and SEM–energy dispersive spectroscopy (EDS) was performed at an acceleration voltage of 15 kV. The samples were first freeze dried at − 48 °C and then coated with platinum by sputtering for 90 s.

Fourier transform infrared (FTIR)-attenuated total reflection (ATR) spectroscopy was performed with a Spectrum Two spectrometer (PerkinElmer, Inc., Waltham, MA) in the range 400–4000 cm^{-1}.

Results and discussion

Preparation and structures

Preparation of the ICN hydrogels

The ICN hydrogels were prepared by in situ polymerization of poly(AM-co-AA) in a CNF cake, followed by ionic cross-linking and equilibration (Fig. 1). In the wet cake, CNF networks with weak interfibrillar interactions form, where exist nanochannels (Koga et al. 2017; Yang et al. 2019). The monomer solution was passed through the CNF cake under vacuum force, reducing the degree of back-mixing. It was a versatile and effective method to replace water inside the CNF cake with various kinds of monomer solutions (Yang et al. 2019). A small amount of covalent cross-linker, MBA, was used to make the poly(AM-co-AA) chains elastic, preventing the resulting hydrogels from having sticky surfaces. Conversion of the monomers was almost 100%, which was confirmed by NMR (Fig. S2). Thus, the poly(AM-co-AA) chains were directly cross-linked by Fe^{3+}, without the process of removing unreacted monomers (Fig. 1d).

Grafting of the polymer chains

It has been reported that polymer chains can be grafted from polysaccharides with persulfate as initiator (Roy et al. 2009; Habibi 2014; Mahfoudhi and Boufi 2016). To confirm the possibility of grafting poly(AM-co-AA) chains from the surface of the CNFs, CNF/poly(AM-co-AA) composite was prepared in the absence of MBA. The resulting sample could be dispersed in water to form a uniform suspension under mild stirring (Fig. S3). Then, the CNFs in sediment were collected by high speed centrifugation (41360 × g, 30 min, 3 times), while the free poly(AM-co-AA) chains, which dissolved in supernatant, were removed completely. As a result, the separated CNFs shows typical poly(AM-co-AA) peaks (blue curve, Fig. 2), which are different with the neat CNFs (black curve, Fig. 2). It was concluded

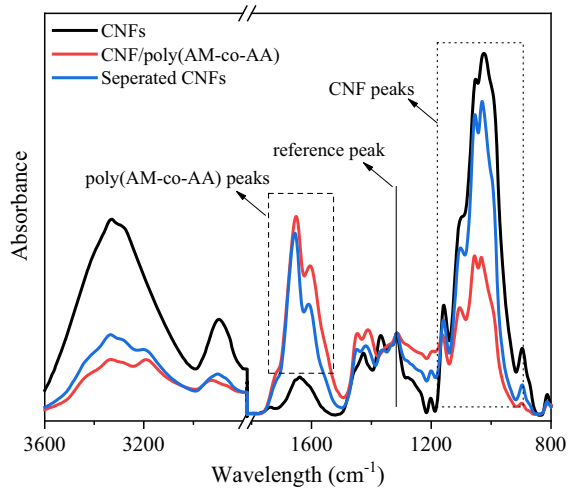

Fig. 2 Normalized FTIR spectra of CNFs, CNF/poly(AM-co-AA) sample prepared in the absence of MBA, and separated CNFs. The reference peak of normalization is at the range between 1316–1315 cm^{-1}

that part of the poly(AM-co-AA) chains were grafted from the surface of the CNFs.

Structures and features of the ICN hydrogels

The macroscopic features of ICN hydrogels are shown in Fig. 3. When one end of CNF/poly(AM-co-AA) hydrogel was fixed, it bent from the fixing point (Fig. 3b), exhibiting the flexible property of poly(AM-co-AA) chains. After ionic cross-linking, the resulting ICN hydrogel became dark brown and rigid owing to the Fe^{3+}/COO^{-} complexes (Fig. 3c, d). The ionic cross-linking was further confirmed by FTIR and SEM–EDS (Fig. S4). Compared with CNF/poly(AM-co-AA) hydrogel, ICN hydrogel slightly shrank in the length direction but shrank by 30% approximately in the thickness direction, leading to a more compact structure. This was because the matrix shrank during ionic cross-linking, resulting in bulk shrinkage. The shrinkage in the thickness direction occurred greatly owing to the relatively loose CNF layers (Fig. S5). In contrast, the shrinkage in the length direction was restrained since the entanglement of CNFs was mainly in-plane. Surprisingly, a small double-fold ICN hydrogel sheet with width of about 1 cm and thickness of 350 μm could sustain the force produced by a 2 kg weight (Fig. 3e). In addition, the ICN hydrogel could be folded into a boat-like shape, showing that the hydrogel is freely foldable (Fig. 3f).

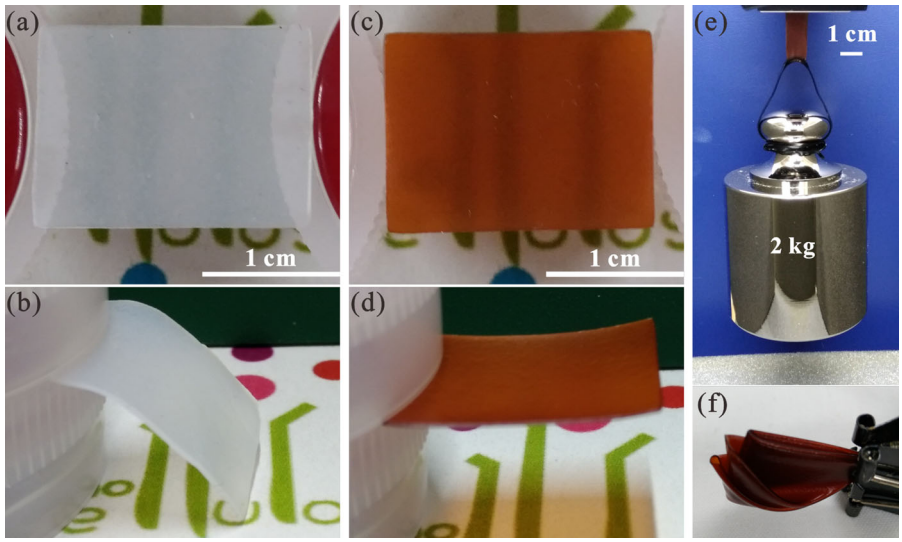

Fig. 3 **a** Photograph of CNF/poly(AM-co-AA) hydrogel. **b** Photograph of one-end-fixed CNF/poly(AM-co-AA) hydrogel. **c** Photograph of an ICN hydrogel. **d** Photograph of a one-end-fixed ICN hydrogel sheet. **e** A small piece of the ICN hydrogel holding a 2 kg weight. **f** Folded ICN hydrogel fixed by a binder clip

Mechanical properties

Role of the CNFs and ionic cross-linking

The effects of CNFs and ionic cross-linking on the mechanical properties were revealed by tensile tests (Fig. 4). When stretched, the as-prepared CNF/poly(AM-co-AA) hydrogel has a low elastic modulus of 1.92 ± 0.31 MPa, a fracture stress of 2.38 ± 0.37 MPa, and elongation of $68.0 \pm 6.0\%$

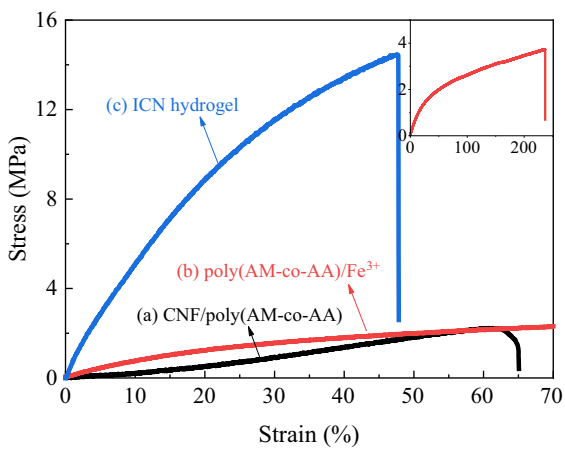

Fig. 4 Stress–strain curves of **a** CNF/poly(AM-co-AA) hydrogel in the absence of ionic cross-linking, **b** poly(AM-co-AA)/Fe^{3+} hydrogel in the absence of CNFs, and **c** the ICN hydrogel. Insert curve: poly(AM-co-AA)/Fe^{3+} hydrogel

(black curve, Fig. 4). On the other hand, Fe^{3+} cross-linked poly(AM-co-AA) hydrogel without using any CNFs, called poly(AM-co-AA)/Fe^{3+}, shows tough properties (red line, Fig. 4). After ionic cross-linking, the ICN hydrogel became much stiffer and stronger without an obvious sacrifice in elongation (blue curve, Fig. 4). Therefore, both the CNFs and ionic cross-linking contributed to mechanical properties. Ionic cross-linking provided rigid polymer chains, improving the interactions between the CNFs and the polymer matrix. The high stiffness and strength of CNFs prevented ICN hydrogel from being stretched and fractured.

Effect of the composition

The effect of ionic cross-linking density and matrix content affected the tensile properties of the ICN hydrogels, which are discussed in detail in this section. First, the MBA content was fixed at 0.1 mol% with respect to the total monomers and the concentration of $FeCl_3$ was fixed at 0.06 M according to preliminary experiments (Fig. S6).

ICN hydrogels with different AA contents were prepared with the total monomer concentration kept constant at 3 mol/L. The ratios of the matrix to the CNFs are all about 2.2 (Table 1). Hydrogels with higher AA content can form more Fe^{3+}/COO^{-}

Table 1 Compositions and mechanical properties of ICN hydrogels

Sample	Compositions				Mechanical properties			
	Water (%)	CNFs (%)	Matrix (%)	Matrix/CNFs	Elastic modulus (MPa)	Elongation (%)	Fracture stress (MPa)	Fracture energy (J/m^2)
AA-8%	75.7	7.6	16.7	2.20	11.92 ± 0.51	66.8 ± 2.5	6.97 ± 0.11	1444.7 ± 273.5
AA-12%	68.9	9.9	21.2	2.14	24.67 ± 1.65	59.8 ± 4.7	9.41 ± 0.19	1420.1 ± 57.7
AA-16%	62.4	11.6	26.0	2.24	53.80 ± 3.86	56.9 ± 1.5	11.74 ± 0.36	1339.4 ± 46.6
AA-20% (3 M)	58.5	13.1	28.4	2.17	95.20 ± 6.50	48.7 ± 2.0	14.18 ± 0.56	1409.4 ± 175.8
AA-24%	51.0	15.0	34.0	2.27	190.03 ± 12.37	38.4 ± 1.6	15.67 ± 0.49	992.6 ± 105.7
1.5-M	75.0	12.3	12.7	1.03	36.46 ± 1.79	40.6 ± 1.1	8.29 ± 0.25	729.1 ± 72.2
2-M	69.2	12.4	18.4	1.48	40.49 ± 3.29	42.2 ± 1.1	9.31 ± 0.10	892.4 ± 71.0
3-M (AA-20%)	58.5	13.1	28.4	2.17	95.20 ± 6.50	48.7 ± 2.0	14.18 ± 0.56	1409.4 ± 175.8
4-M	54.3	11.4	34.3	3.01	104.29 ± 6.42	51.2 ± 1.7	16.53 ± 0.30	2325.6 ± 6.4
5-M	52.4	10.5	37.1	3.53	102.30 ± 6.88	49.7 ± 2.7	17.15 ± 0.16	2492.8 ± 63.81

For easy comparison, entries 4 and 8 are the same sample with different names

complexes, squeezing more water out of the poly(AM-co-AA) networks and making the networks more compact. With increasing AA content, elongation gradually decreases while the elastic modulus and fracture strength increase. The AA-24% sample has an elastic modulus of 190.03 ± 12.37 MPa (Table 1 and Fig. 5a). The fracture energy is about 1400 J/m^2 when the AA ratio is less than 24%. This could be because the enhanced stiffness offsets the decrease in the critical strain. The fracture energy of AA-24% decreases to 992.6 ± 105.7 J/m^2 owing to the large decrease in the critical strain.

The effect of the total monomer content on the mechanical properties was investigated. When the concentration of total monomers is increased from 1.5 to 3 M, the water content rapidly decreases from 75.0% to 58.5%, while the poly(AM-co-AA)/Fe^{3+} content shows the opposite trend (entries 6–10, Table 1). The CNF content slightly increases from 12.3% to 13.1%. When the total monomer concentration is less than 3 mol/L, the ICN hydrogels show relatively soft and weak properties. When the total monomer concentration is further increased to 5 M, the water content slightly decreases to 52.4%, the poly(AM-co-AA)/Fe^{3+} content increases to 37.1%, and the CNF content decreases to 10.5%. The tensile properties also slightly change (Fig. 5b) while the highest fracture energy of 2492.8 ± 63.8 J/m^2 is achieved for 5-M (Table 1). Noting that the mole ratio of the initiator to the monomers was fixed at 0.1%, 5-M may have more grafted polymer chains, contributing to the toughness.

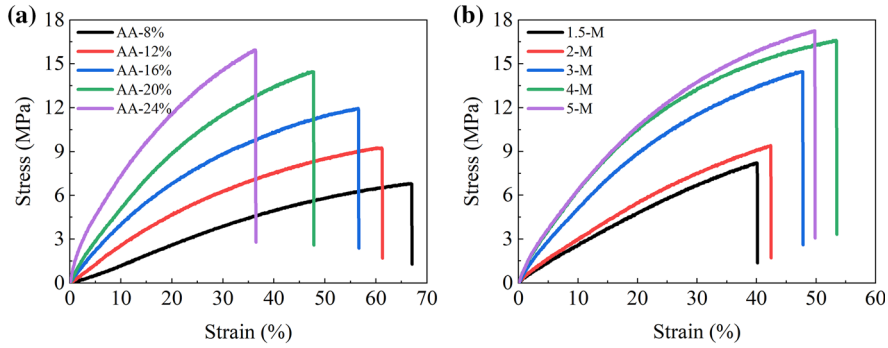

Fig. 5 Tensile stress–strain curves of ICN hydrogels with different AA ratios (**a**) and different monomer concentrations (**b**)

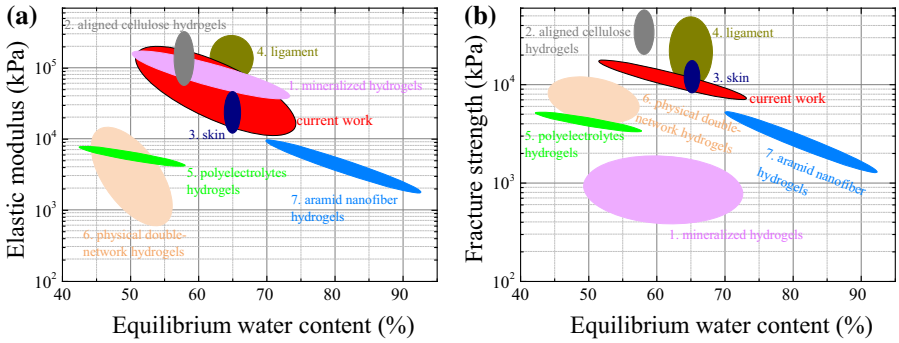

Fig. 6 Comparison of the ICN hydrogels with typical stiff and strong hydrogels and soft tissues. **a** Elastic modulus versus equilibrium water content. **b** Fracture strength versus equilibrium water content. The data are adapted from the literature: 1. mineralized hydrogel (Rauner et al. 2017), 2. aligned cellulose hydrogel (Mredha et al. 2018), 3 and 4. skin and ligament (Wegst and Ashby 2004; Dubinskaya et al. 2007), 5. polyelectrolytes hydrogel (Luo et al. 2015), 6. physical double-network hydrogel (Zhang et al. 2016), and 7. aramid nanofiber hydrogel (Xu et al. 2018)

For the tensile properties, the ICN hydrogels show both stiff and strong properties compared with some recently developed hydrogels (Fig. 6) (Mredha et al. 2018; Rauner et al. 2017; Luo et al. 2015; Zhang et al. 2016; Xu et al. 2018). In addition, the elastic moduli, fracture strengths, and water contents of the ICN hydrogels are comparable with those of some soft tissues (Fig. 6) (Wegst and Ashby 2004; Dubinskaya et al. 2007).

Fracture mechanism

Different with a single CNF or dried CNF films, wet CNF films do not guarantee good tensile properties owing to dissociation of interfibrillar hydrogen bonds in wet conditions (De France et al. 2017; Benitez et al. 2013; Yang et al. 2018). In addition, ground CNFs with widths of around 15 nm and lengths of several micrometers are not continuous nanofibers (Abe et al. 2007), promoting the pull-out mechanism in the hydrated state (Benitez et al. 2013). Consequently, the wet CNF cake was too soft and weak for tensile tests. After in situ polymerization, the tensile properties of the CNF/poly(AM-co-AA) hydrogel are superior to those of the CNF cake. The good affinity between the CNFs and poly(AM-co-AA), resulting from polymer grafting, hydrogen bonds, and entanglement, improves the mechanical properties. However, the CNF/poly(AM-co-AA) structure is not sufficiently compact and the poly(AM-co-AA) chains are very soft, inhibiting further increase of the stiffness and strength. After ionic cross-linking and equilibration in water, the poly(AM-co-AA) matrix shrinks and becomes stiffer, greatly enhancing the frictional force between the CNFs and the matrix. Therefore, the elastic moduli of the ICN hydrogels are extremely high and can be easily adjusted by controlling the ionic cross-linking density.

At the same time, because the CNFs are surrounded by a polymer matrix, the direct interactions between the CNFs are weak, which is different from the CNF-only hydrogels (Abe and Yano 2012). Therefore, the random CNFs may be orientated during stretching, which prevents failure of the bulk hydrogel. As a result, ICN hydrogels are stretchable and elongation is dependent on the ionic cross-linking density and matrix content (Fig. 5). A high ionic cross-linking density inhibits orientation of the CNFs before fracture of the bulk hydrogel (Fig. 5a), but a suitable matrix content facilitates orientation of the CNFs (Fig. 5b). Thus, the extremely stiff ICN hydrogels with good stretchability also possess high strength comparable with real tissues (Fig. 6). On the other hand, the fiber strength is higher than the frictional force that the CNF/matrix can sustain. When the tensile stress reaches the maximum frictional force, CNFs are pulled out and fracture of the bulk hydrogel occurs. SEM images of the fracture surface show pull-out phenomena at multiple length scales (Fig. 7), which is similar to fracture of CNF film at 100% relative humidity (Benitez et al. 2013). Many individual nanofibers remain on the fracture surface (white arrows, Fig. 7b) and small pores with diameters of several tens of nanometers are also observed (red

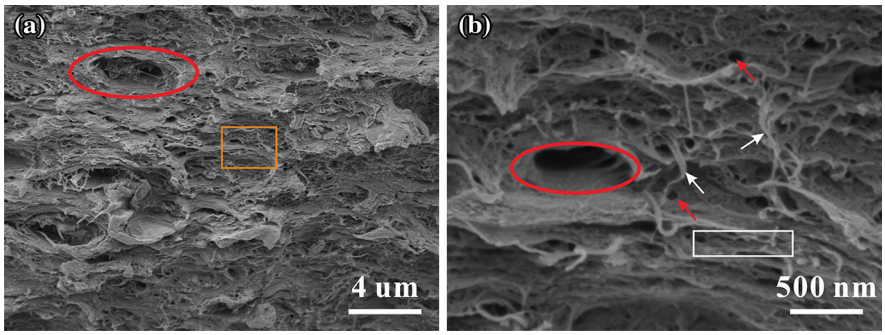

Fig. 7 Freeze-dried fracture surface of the ICN hydrogels. **a** Low magnification. **b** High magnification of the orange rectangle-marked area in (**a**)

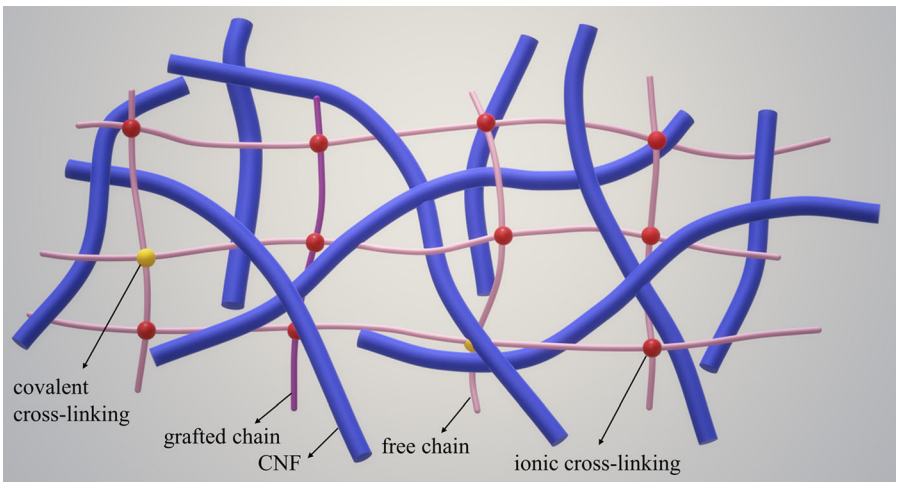

Fig. 8 Schematic description of the ICN hydrogels

arrows, Fig. 7b). On a larger scale, some CNF layers produced during filtration can be pulled out (white rectangle, Fig. 7b). In addition, CNF aggregation and floc, which are induced by filtration (Benitez et al. 2013), are pull out as a whole (red ellipses, Fig. 7a, b). Therefore, we conclude that pull-out is probably the main fracture mechanism. We also propose the structures of the ICN hydrogels (Fig. 8). The CNFs are surrounded by the polymer matrix and part of polymer chains are grafted from the surfaces of the CNFs. In the current study, the degree of grafting was not controlled and the effect of the grafting density on tensile properties needs further investigation in the future study. Polymer chains are dually cross-linked by covalent bonds and ionic bonds.

As mentioned in our previous report (Yang et al. 2018), combining layered CNFs with strong and tough polymer networks can result in nanocomposite hydrogels with good mechanical properties. Therefore, we predict that various other polymer networks are suitable for fabricating CNF/polymer hydrogels with good mechanical properties or/and different features by the method of in situ polymerization.

Conclusion

We in situ polymerized the poly(AM-co-AA) matrix in a wet CNF cake, after which ironical cross-linking was performed. The elastic moduli of the resulting hydrogels are extremely high owing to the enhanced friction force between CNFs and ionically cross-linked polymer matrix. In addition, CNF/polymer nanocomposite hydrogels with high CNF content and good stretchability are simultaneously reached by reducing the direct interfibrillar interactions. We predict that various types of polymer networks could be incorporated into the CNF cake to achieve good mechanical properties and/or different features.

References

Abe K, Yano H (2009a) Comparison of the characteristics of cellulose microfibril aggregates isolated from fiber and parenchyma cells of Moso bamboo (Phyllostachys pubescens). Cellulose 17(2):271–277. https://doi.org/10.1007/s10570-009-9382-1

Abe K, Yano H (2009b) Comparison of the characteristics of cellulose microfibril aggregates of wood, rice straw and potato tuber. Cellulose 16(6):1017–1023. https://doi.org/10.1007/s10570-009-9334-9

Abe K, Yano H (2012) Cellulose nanofiber-based hydrogels with high mechanical strength. Cellulose 19(6):1907–1912. https://doi.org/10.1007/s10570-012-9784-3

Abe K, Iwamoto S, Yano H (2007) Obtaining cellulose nanofibers with a uniform width of 15 nm from wood. Biomacromol 8(10):3276–3278

Benitez AJ, Torres-Rendon J, Poutanen M, Walther A (2013) Humidity and multiscale structure govern mechanical properties and deformation modes in films of native cellulose nanofibrils. Biomacromol 14(12):4497–4506. https://doi.org/10.1021/bm401451m

Chen C, Li D, Abe K, Yano H (2018) Formation of high strength double-network gels from cellulose nanofiber/polyacrylamide via NaOH gelation treatment. Cellulose. https://doi.org/10.1007/s10570-018-1938-5

De France KJ, Hoare T, Cranston ED (2017) A review of hydrogels and aerogels containing nanocellulose. Chem Mater 29(11):4609–4631. https://doi.org/10.1021/acs.chemmater.7b00531

Dubinskaya VA, Eng LS, Rebrow LB, Bykov VA (2007) Comparative study of the state of water in various human tissues. Bull Exp Biol Med 144(3):294–297. https://doi.org/10.1007/s10517-007-0314-5

Gong JP (2010) Why are double network hydrogels so tough? Soft Matter 6(12):2583. https://doi.org/10.1039/b924290b

Habibi Y (2014) Key advances in the chemical modification of nanocelluloses. Chem Soc Rev 43(5):1519–1542. https://doi.org/10.1039/c3cs60204d

Hu Y, Du Z, Deng X, Wang T, Yang Z, Zhou W et al (2016) Dual physically cross-linked hydrogels with high stretchability, toughness, and good self-recoverability. Macromolecules 49(15):5660–5668. https://doi.org/10.1021/acs.macromol.6b00584

Klemm D, Kramer F, Moritz S, Lindstrom T, Ankerfors M, Gray D et al (2011) Nanocelluloses: a new family of nature-based materials. Angew Chem Int Ed Engl 50(24):5438–5466. https://doi.org/10.1002/anie.201001273

Kobe R, Iwamoto S, Endo T, Yoshitani K, Teramoto Y (2016) Stretchable composite hydrogels incorporating modified cellulose nanofiber with dispersibility and polymerizability: mechanical property control and nanofiber orientation. Polymer 97:480–486. https://doi.org/10.1016/j.polymer.2016.05.065

Koga H, Namba N, Takahashi T, Nogi M, Nishina Y (2017) Renewable wood pulp paper reactor with hierarchical micro/nanopores for continuous-flow nanocatalysis. Chemsuschem 10(12):2560–2565. https://doi.org/10.1002/cssc.201700576

Li J, Illeperuma WRK, Suo Z, Vlassak JJ (2014) Hybrid hydrogels with extremely high stiffness and toughness. ACS Macro Lett 3(6):520–523. https://doi.org/10.1021/mz5002355

Lin P, Ma S, Wang X, Zhou F (2015) Molecularly engineered dual-crosslinked hydrogel with ultrahigh mechanical strength, toughness, and good self-recovery. Adv Mater 27(12):2054–2059. https://doi.org/10.1002/adma.201405022

Lin P, Zhang T, Wang X, Yu B, Zhou F (2016) Freezing molecular orientation under stretch for high mechanical strength but anisotropic hydrogels. Small 12(32):4386–4392. https://doi.org/10.1002/smll.201601893

Luo F, Sun TL, Nakajima T, Kurokawa T, Zhao Y, Sato K et al (2015) Oppositely charged polyelectrolytes form tough, self-healing, and rebuildable hydrogels. Adv Mater 27(17):2722–2727. https://doi.org/10.1002/adma.201500140

Mahfoudhi N, Boufi S (2016) Poly (acrylic acid-co-acrylamide)/cellulose nanofibrils nanocomposite hydrogels: effects of CNFs content on the hydrogel properties. Cellulose 23(6):3691–3701. https://doi.org/10.1007/s10570-016-1074-z

Meyers MA, Chen P-Y, Lin AY-M, Seki Y (2008) Biological materials: structure and mechanical properties. Prog Mater Sci 53(1):122

Mredha MTI, Guo YZ, Nonoyama T, Nakajima T, Kurokawa T, Gong JP (2018) A facile method to fabricate anisotropic hydrogels with perfectly aligned hierarchical fibrous structures. Adv Mater 30(9):1704937. https://doi.org/10.1002/adma.201704937

Nascimento DM, Nunes YL, Figueirêdo MCB, de Azeredo HMC, Aouada FA, Feitosa JPA et al (2018) Nanocellulose nanocomposite hydrogels: technological and environmental issues. Green Chem 20(11):2428–2448. https://doi.org/10.1039/c8gc00205c

Oyen ML (2013) Mechanical characterisation of hydrogel materials. Int Mater Rev 59(1):44–59. https://doi.org/10.1179/1743280413y.0000000022

Rauner N, Meuris M, Zoric M, Tiller JC (2017) Enzymatic mineralization generates ultrastiff and tough hydrogels with tunable mechanics. Nature 543(7645):407–410. https://doi.org/10.1038/nature21392

Roy D, Semsarilar M, Guthrie JT, Perrier S (2009) Cellulose modification by polymer grafting: a review. Chem Soc Rev 38(7):2046–2064. https://doi.org/10.1039/b808639g

Wang W, Zhang Y, Liu W (2017) Bioinspired fabrication of high strength hydrogels from non-covalent interactions. Prog Polym Sci 71:1–25. https://doi.org/10.1016/j.progpolymsci.2017.04.001

Wegst UGK, Ashby MF (2004) The mechanical efficiency of natural materials. Phil Mag 84(21):2167–2186. https://doi.org/10.1080/14786430410001680935

Xu L, Zhao X, Xu C, Kotov NA (2018) Water-rich biomimetic composites with abiotic self-organizing nanofiber network. Adv Mater 30(1):1703343. https://doi.org/10.1002/adma.201703343

Yang XP, Abe K, Biswas SK, Yano H (2018) Extremely stiff and strong nanocomposite hydrogels with stretchable cellulose nanofiber/poly(vinyl alcohol) networks. Cellulose 25(11):6571–6580. https://doi.org/10.1007/s10570-018-2030-x

Yang XP, Biswas SK, Yano H, Abe K (2019) Stiffened nanocomposite hydrogels by using modified cellulose nanofibers via plug flow reactor method. ACS Sustain Chem Eng 7(10):9092–9096. https://doi.org/10.1021/acssuschemeng.9b01322

Zhang YS, Khademhosseini A (2017) Advances in engineering hydrogels. Science 356(6337):eaaf3627. https://doi.org/10.1126/science.aaf3627

Zhang HJ, Sun TL, Zhang AK, Ikura Y, Nakajima T, Nonoyama T et al (2016) Tough physical double-network hydrogels based on amphiphilic triblock copolymers. Adv Mater 28(24):4884–4890. https://doi.org/10.1002/adma.201600466

Zhao X (2017) Designing toughness and strength for soft materials. Proc Natl Acad Sci 114(31):8138–8140

Zheng SY, Ding H, Qian J, Yin J, Wu ZL, Song Y et al (2016) Metal-coordination complexes mediated physical hydrogels with high toughness, stick-slip tearing behavior, and good processability. Macromolecules 49(24):9637–9646. https://doi.org/10.1021/acs.macromol.6b02150